

Parameter estimation of synchronous machines considering field voltage variation during the sudden short-circuit test

Victor A.D. Faria, J.V. Bernardes Jr, Edson C. Bortoni

Center of Excellence in Energy Efficiency, Federal University of Itajubá, Itajubá, MG 37500-903, Brazil

ARTICLE INFO

Keywords:

Optimization models
Field voltage variation
Parameter identification
Sudden three-phase short-circuit test
Synchronous machines

ABSTRACT

This work examines the influence of field voltage variation during a sudden short-circuit test and its direct impact on the parameter identification of synchronous machines. The test standards establish that field voltage must be kept constant during the short-circuit test. However, due to the presence of impedances in the voltage supply, control of the excitation system along with many other factors, field voltage may vary during this test. This work proposes a method to recover the machine parameters even when high amplitude field voltage variations are presented during the sudden short-circuit test. In addition, an algorithm capable of defining maximum field voltage variations along with its correspondent duration in order to respect a certain parameter estimation error is proposed. Finally, the models developed in this paper are investigated using data from a 140 MVA synchronous machine.

1. Introduction

Presently, almost all electrical power generated in the world comes from synchronous generators. Mathematically, this machine is usually modeled using the Park transform [1], which allows its representation as two equivalent circuits and simplify several times the differential equations that govern the behavior of this machine.

Knowledge of the direct-axis and quadrature-axis equivalent circuit parameters play an important role in studies of transient stability, small signal stability, faults protection, and sub-synchronous resonance [2–4].

There are several methods to determine the parameters of synchronous machines. Such methods include: standstill frequency response, load rejection, voltage recovery test, and sudden short-circuit test [5–9].

The sudden three-phase short-circuit is an accepted test frequently used in the parameter identification of synchronous machines. This method has been used for more than 80 years and consists in applying a solid three-phase short-circuit on the machine terminals with the machine on open circuit. The field excitation voltage must be kept constant during the decay of the three-phase fault currents to steady-state values. With the short-circuit test, it is possible to determine d-axis parameters by analyzing the armature currents [5].

The IEEE Std. 115 provides special emphasis to the care that must be taken in order to avoid significant field voltage variations, especially during the load rejection, voltage recovery, and short-circuit tests.

It is recommended that the excitation system be supplied by a constant-voltage low-impedance source, which may require an independent excitation system different from the one used during normal service. Also, the voltage regulator must be set to manual control [5].

The subject of field voltage variation while performing d-axis parameters identification tests is poorly discussed in the technical literature. The work presented in [10] touches on this subject when considering field-voltage source impedance in the parameters calculation. Also, IEEE Std. 115 mentions an exceptional situation in which the load rejection test is performed on a machine where the excitation system is fed from the generator terminals. In this case, the IEEE Std. 115 states that the dynamic of the field voltage should be taken into consideration during the parameters derivation process [5]. However, no explanation is given on how to incorporate this dynamic in the parameters identification. Ref. [11] fills this gap.

Noticing the gaps that exist in the understanding of the effects that field voltage variation can bring to the parameter identification of synchronous machines, this work presents a mathematical modeling of the sudden three-phase short-circuit test considering field voltage variation during the short-circuit transient.

E-mail addresses: duraes_victor@unifei.edu.br (V.A.D. Faria), jusevitor@unifei.edu.br (J.V. Bernardes), bortoni@unifei.edu.br (E.C. Bortoni).

<https://doi.org/10.1016/j.ijepes.2019.105421>

Received 30 January 2019; Received in revised form 22 April 2019; Accepted 16 July 2019

0142-0615/ © 2019 Elsevier Ltd. All rights reserved.

Nomenclature

$G(s)$	transfer function that relates the stator flux linkages per second with field voltage (p.u.)
i_f	instantaneous value of the field current (p.u.)
$i(t)$	instantaneous value of the a -phase short-circuit current with or without field voltage variations (p.u.)
$i_{NV}(t)$	instantaneous value of the a -phase short-circuit current with no field voltage variations (p.u.)
$i_{T_i}^{\Delta f}(t)$	instantaneous value of the a -phase short-circuit current due to a step in the field voltage applied in a given time (p.u.)
N_s	number of samples of the armature current.
N_t	number of field voltage drop time intervals
N_v	number of field voltage drop magnitudes
r_a	phase armature winding resistance (p.u.)
$SC(t)$	AC RMS value of the measured current during the short-circuit test at an instant t (p.u.)
t_i	i -th time sample (s)
T_{fdp}	maximum duration of a field voltage drop (s)
T_i	instant that the step i is applied in the field voltage (s)
$U(T)$	unit step function applied in $t = T$
v_f	instantaneous value of the field voltage (p.u.)

V_{f0}	field voltage prior to the short-circuit (p.u.)
V_{fdp}	maximum field voltage drop (p.u.)
$V_{\Delta f}(T_i)$	amplitude of the field voltage step applied in T_i (p.u.)
V_s	line to neutral RMS value of the armature voltage prior to the short-circuit (p.u.)
x_a	leakage stator reactance (p.u.)
$X_d(s)$	d-axis operational impedance (p.u.)
x_{kf}	mutual damper to field windings reactance (p.u.)
x_{md}	d-axis armature mutual reactance (p.u.)
x_{mq}	q-axis armature mutual reactance (p.u.)
$X_q(s)$	q-axis operational impedance (p.u.)
$\Delta V_{d,q,f}$	Laplace transform applied to the difference between the instantaneous value of the voltage v_d , v_q or v_f and its correspondent steady-state value
$\Delta I_{d,q}$	Laplace transform applied to the difference between the instantaneous value of the current i_d or i_q and its correspondent steady-state value
α	inverse of the armature time constant (s^{-1})
$\gamma_{0,d,q}$	zero-sequence (γ_0), d-axis (γ_d), and q-axis (γ_q) component of the γ quantity
$\gamma_{a,b,c}$	stator phase components of the a (γ_a), b (γ_b), and c (γ_c) windings of the γ quantity
$\mathcal{L}^{-1}\{\cdot\}$	inverse laplace transform

Two mathematical models are proposed to recover the machine parameters. The first one considers the traditional constant field voltage condition while attempting to estimate the machine parameters by using interpolation methods over the armature current, the Constant Field Voltage Interpolation (CFVI). The second method uses the equations developed in the appendix, which considers field voltage variation in its formulation, the Variable Field Voltage Interpolation (VFVI).

The CFVI represents the method used nowadays in the recovery of the machine parameters from short-circuit tests. On the other hand, the VFVI is an alternative developed in this article to recover the machine parameters from short-circuit tests with field voltage variations.

Finally, for the CFVI, this paper derives the maximum field voltage variations along with its correspondent durations, to respect a defined parameter estimation error.

This paper is divided as follows: Section 2 explains the equations that govern the sudden short-circuit test with and without field voltage variations. Section 3 describes the models developed in order to interpolate the armature current of the short-circuit test with and without field voltage variation, and in this way, recover the machine parameters in both cases. Section 4 presents an algorithm to compute limits of field voltage variation for a given maximum admissible error in the parameter estimation. Section 5 presents a study using data from a 140 MVA synchronous machine. The appendix provides a formal mathematical proof of the equations used to model the sudden short-circuit test with field voltage variation.

2. Sudden short-circuit mathematical model

During the short-circuit test when the field voltage is kept constant, and a solid three-phase short-circuit is applied in an unloaded synchronous machine, it is possible to prove that the armature current can be described by (1) [12].

As stated in IEEE Std. 115 [5], the short-circuit test has to be performed using a constant voltage, low-impedance source of excitation in order to avoid errors in the determination of the machine parameters due to field voltage variations that are not considered in the formulations presented in this standard. The remainder of this section, however, models the short-circuit considering the field voltage variation phenomenon.

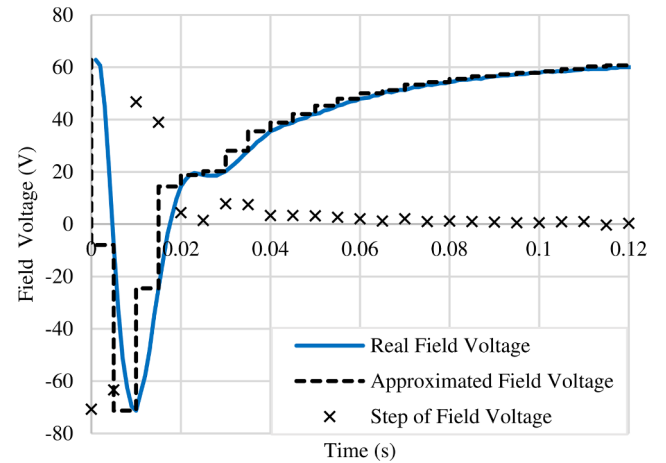


Fig. 1. Approximation of the field voltage variation.

$$\begin{aligned}
 i_{NV}(t) = & \sqrt{2} V_s \left[\frac{1}{x_d} + \left(\frac{1}{x'_d} - \frac{1}{x_d} \right) e^{-\frac{t}{\tau'_d}} \right] \sin(\omega t + \theta_0) \\
 & + \sqrt{2} V_s \left(\frac{1}{x'_d} - \frac{1}{x_d} \right) e^{-\frac{t}{\tau'_d}} \sin(\omega t + \theta_0) \\
 & - \frac{\sqrt{2}}{2} V_s \left(\frac{1}{x'_d} + \frac{1}{x'_d} \right) e^{-\alpha t} \sin(\theta_0) \\
 & - \frac{\sqrt{2}}{2} V_s \left(\frac{1}{x'_d} - \frac{1}{x'_q} \right) e^{-\alpha t} \sin(2\omega t + \theta_0)
 \end{aligned} \quad (1)$$

Fig. 1 describes a measured field voltage variation during a short-circuit test. Represented by a continuous line, this field voltage variation can be approximated by the sum of step functions represented by dashed lines. Also, in Fig. 1, the amplitudes and instant that each step of field voltage is applied are denoted by an 'x' mark. The amplitude of the step applied in T_i ($V_{\Delta f}(T_i)$) is the difference between the field voltage measured in $T_i + \Delta t$ and T_i ; where Δt is the time interval between two consecutive step functions. From this perspective, $V_{\Delta f}(T_i)$ can be positive or negative depending on whether the field voltage is decreasing or increasing in a given Δt .

The field variation presented in Fig. 1 was obtained from a short-circuit test with the same settings presented in [13], where an

impedance was deliberately placed in series with the field circuit to intensify the field voltage variation.

Note that Fig. 1 is only an illustrative example and is not intended to present a recurrent field voltage variation from a short-circuit test.

In the remainder of this section, the field voltage variation is approximated by the sum of step functions. As proved in the appendix, this approximation allows obtaining a simple expression that relates the field voltage variations with the armature short-circuit currents.

Eq. (2) is deduced in the appendix and relates the armature current with a single step in the field voltage applied in a short-circuited synchronous machine initially with no field voltage and rotating at synchronous speed.

$$i_{Ti}^{df}(t) = \sqrt{\frac{2}{3}} \frac{x_{md} V_{df}(T_i)}{x_d r_f} \left(1 - e^{-\frac{t-T_i}{\tau_d}} \right) \sin(\omega t + \theta_0) U(T_i) \quad (2)$$

As proved in the appendix, the individual impact of a step of field voltage variation only depends on the rotor speed prior to the application of this step. By assuming a constant rotor speed during the test, it is possible to sum the individual influence of each step in the field voltage. Finally, the short-circuit current during a test with field voltage variation can be described by (3).

The intuition behind (3) is that a momentaneous decrease in the field voltage ($V_{df}(T_i) < 0$) implies in a subtraction of the original current $i_{NV}(t)$; on the other hand, as the field voltage starts to increase again the new steps of field voltage would have $V_{df}(T_i) > 0$, reverting the distortion previously imposed when $V_{df}(T_i) < 0$.

$$i(t) = i_{NV}(t) + \sum_{i=1}^{N_s} i_{Ti}^{df}(t) \quad (3)$$

In (2), the relation x_{md}/r_f can be obtained before the short-circuit is applied (4), by using the initial machine conditions and the Eqs. (a1) to (a13).

$$\frac{x_{md}}{r_f} = \sqrt{3} \frac{V_s}{V_{f0}} \quad (4)$$

By neglecting the second harmonic of the armature current, it is possible to write (1) in terms of its AC RMS component (5). Additionally, while neglecting the second harmonic of (1), there is no phase shift between (1) and (2) thus the AC RMS component of (3) can be written as (6).

$$I_{NV}(t) = V_s \left[\frac{1}{x_d} + \left(\frac{1}{x_d'} - \frac{1}{x_d} \right) e^{-\frac{t}{\tau_d'}} + \left(\frac{1}{x_d''} - \frac{1}{x_d'} \right) e^{-\frac{t}{\tau_d''}} \right] \quad (5)$$

$$I(t) = I_{NV}(t) + \frac{V_s}{x_d} \sum_{i=1}^{N_s} \frac{V_{df}(T_i)}{V_{f0}} \left(1 - e^{-\frac{t-T_i}{\tau_d}} \right) U(T_i) \quad (6)$$

Given that (6) is a good approximation of the behavior of the armature current when a machine is facing a short-circuit test under field voltage variation, this equation can be used to recover the machine parameters if the field voltage is recorded during the test. Also, (6) can be used to perform a sensitivity analysis of the parameters determined by the short-circuit test in the face of field voltage variations.

3. Models to recover the machine parameters from sudden short-circuit tests

3.1. Parameters identification

The traditional d-axis parameters of synchronous machines are estimated from the AC RMS components of the armature currents in the short-circuit test, which are obtained after extracting the DC unidirectional components. IEEE Std. 115 suggests to subtract from the measured AC RMS armature current the steady state current after the short-

circuit (V_s/x_d), plotting the resultant data in a semi-log scale. This procedure allows linearization in two main regions, transient and sub-transient [5].

However, the results of this method are significantly dependent on how the test data are interpreted [5,14]. In order to avoid subjectivity in the identification of the machine parameters, this paper makes a nonlinear regression over the AC RMS component of the armature current.

There are several methods in the literature that could be used to support the nonlinear regression in the estimation of the machine parameters from the short-circuit current. A particle swarm optimization method [15,16], a genetic algorithm [17] or even a simple and straightforward gradient descent method could all be used. However, as far as the authors know, there is no algorithm capable of guaranteeing global optima for the nonlinear regression of the current in the sudden short-circuit test.

Here, the nonlinear regression of the AC RMS component of the armature current during the short-circuit test was implemented in AMPL [18] using the optimization solver Knitro [19]. Knitro is a well-known tool with several useful features. For example, it has a multi-start procedure for finding high-quality locally optimal solutions to nonconvex problems. It also allows constraints to be incorporated in the optimization process and has several embedded algorithms being able to select the best option based on the problem characteristics.

Considering that the parameters x_d and x_d'' depend only on long-term and initial and currents, respectively, and are not influenced by the field voltage variation, yields (8) to (9).

The variables x_d' , τ_d' , and τ_d'' are obtained by solving the optimization model (7) to (12). In (10) to (12) the subscript *min* and *max* indicate lower bounds and upper bounds for the machine parameters, respectively. The intervals of (10) to (12) can be substituted by any intervals where the variables x_d' , τ_d' , and τ_d'' can be determined with some level of confidence.

In this work, these intervals were chosen as $\pm 50\%$ of the parameter values provided by the manufacturer.

$$\text{Min} \sum_{i=1}^{N_s} [SC(t_i) - I_{NV}(t_i)]^2 \quad (7)$$

s. t.

$$x_d = \frac{V_s}{SC(\infty)} \quad (8)$$

$$x_d'' = \frac{V_s}{SC(0)} \quad (9)$$

$$x_{dmin}' \leq x_d' \leq x_{dmax}' \quad (10)$$

$$\tau_{dmin}' \leq \tau_d' \leq \tau_{dmax}' \quad (11)$$

$$\tau_{dmin}'' \leq \tau_d'' \leq \tau_{dmax}'' \quad (12)$$

The objective function aims to minimize the absolute distance between the measured current $SC(t)$ and the theoretical current $I_{NV}(t)$. Constraints (8) and (9) state that x_d and x_d'' are not variables of the problem. Constraints (10) to (12) are not necessary to the optimization model, but they help the optimization algorithm converge faster and to more accurate values since they decrease the feasibility region of the problem.

In the next sections, the model (7) to (12) is referred to as CFVI, and the model (7) to (12) substituting (7) by (13) is referred to as VFVI.

$$\text{Min} \sum_{i=1}^{N_s} [SC(t_i) - I(t_i)]^2 \quad (13)$$

In this paper, the CFVI model is treated as the current state of the art for recovering the machine parameters from the short-circuit current.

On the other hand, the VFVI model is a new approach developed in this paper to recover the machine parameters from short-circuit tests that faced field voltage variations.

3.2. Limitations and considerations

The CFVI and VFVI models described previously use the AC RMS component of the armature current during the short-circuit to recover the traditional d-axis machine parameters. This AC RMS component is obtained by subtracting the upper envelope and the lower envelope of the armature current and dividing the result by two times the square root of two. These envelopes are usually obtained doing a spline interpolation or polynomial fitting over the short-circuit current and are mainly based on the peak values of the armature current [5,14].

For machines with small d-axis time constants, which are usually small machines, the transient and sub-transient periods happen fast. Also, any field voltage variation has the potential to impact the armature current since, according to (2), if τ_d is small, $i_n^{df}(t)$ can assume its maximum value faster. For this type of machine, if a field voltage variation happens during two peaks of the short-circuit current, the AC RMS component of the armature current obtained by the envelope method may not carry the information of the field voltage variation between the two peaks.

In this condition, the interpolation methods that use the AC RMS component of the short-circuit current (5) to (6) would not be able to recover the machine parameters properly.

An alternative is to carry out an interpolation over the instantaneous value of the armature current using (3). This would, however, represent a challenge given the high nonlinearity and complexity of (3).

4. Computing limits of field voltage variation given a maximum admissible error

The objective of this section is to propose an algorithm capable of defining limits of field voltage variation in order to respect a maximum admissible error during the estimation of x_d' , τ_d' , and τ_d'' , while using the CFVI model.

Fig. 2 shows how the algorithm developed in this paper works. As input, the algorithm receives the field voltage V_{f0} that is applied to the machine prior to the short-circuit, a maximum field voltage drop (V_{fdp}), and a maximum duration of this drop (T_{fdp}). The values V_{fdp} and T_{fdp} are used to construct different field voltage curves, that are going to be investigated by the algorithm. In order to construct these curves, V_{fdp} is divided in N_v intervals (14) and T_{fdp} in N_t intervals (15). Finally, the field voltage curves investigated are proposed as in (16).

$$\Delta FV = \frac{V_{fdp}}{N_v} \quad (14)$$

$$\Delta t = \frac{T_{fdp}}{N_t} \quad (15)$$

$$v_f(t) = V_{f0} - k\Delta FV [U(0) - U(n\Delta t)] \quad n \in \{1, \dots, N_t\}; k \in \{1, \dots, N_v\} \quad (16)$$

Using the machine parameters provided by the manufacturer as the reference values (x_{d_r} , x_{d_r}' , x_{d_r}'' , τ_{d_r} , and τ_{d_r}''), and the voltage profiles described in (16), the AC component of the RMS current in the armature during a three-phase sudden short-circuit test can be obtained by solving the appendix Eqs. (a1) to (a13) and by using the envelope method over the solution [1].

Usually, to solve the model (a1) to (a13) for each $v_f(t)$ profile (16) requires a significant computational effort mainly for two reasons. First, the model (a1) to (a13) are a set of differential equations that need to be solved numerically from time zero to the steady state condition and second, the number of $v_f(t)$ profiles can be large depending of the N_t

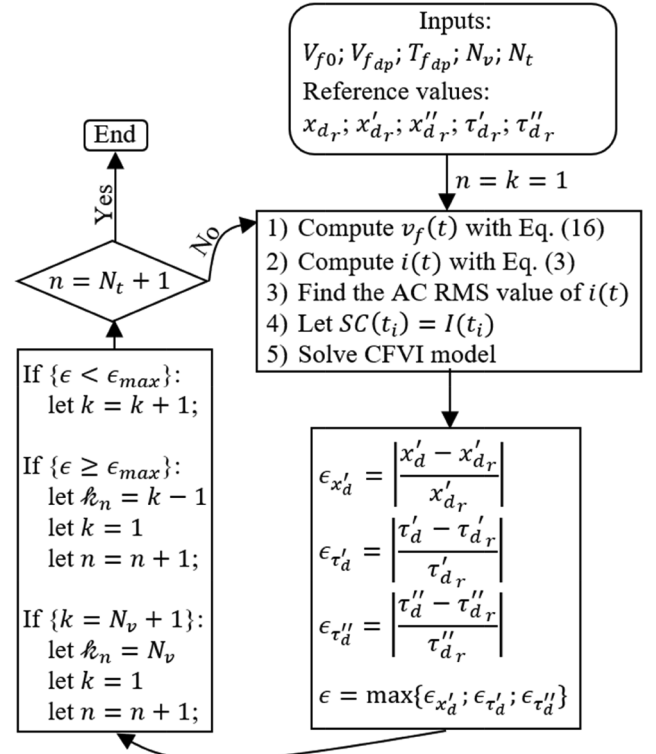


Fig. 2. Description of the algorithm that computes limits of field voltage variation given a maximum admissible error.

and N_v values. However, as will be shown in the numerical results section, (3) is an excellent approximation for the phenomenon investigated here. This way, (3) is going to be used to compute the armature current for each $v_f(t)$ profile.

Fig. 3 is a schematic of how the algorithm of Fig. 2 investigates different limits for the field voltage variation. For each integer $n \in \{1, \dots, N_t\}$, the algorithm searches for the larger $k \in \{1, \dots, N_v\}$ where using the CFVI model an error smaller than a preset value ϵ_{max} is obtained for the x_d' , τ_d' , and τ_d'' parameters. This k value is going to be denoted as k_n .

Knowing k_n for each corresponding iteration n , it is possible to define an approximate region where the field voltage can vary without compromising the determination of the machine parameters with an error larger than ϵ_{max} .

It is important to note that the algorithm developed in this section (Fig. 2) is an approximation since, in order to construct the

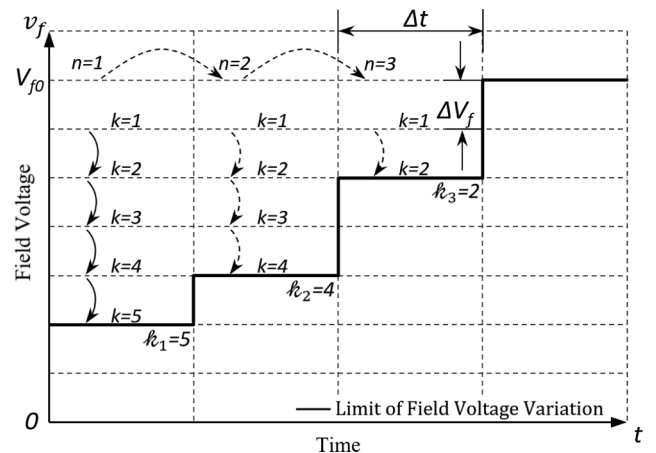


Fig. 3. Progression of the algorithm that computes the field voltage limits.

forementioned region (Fig. 3) it was considered that the voltage drop could be represented by only two step functions, one applied in $t = 0$, and the other in $t = n\Delta t$. However, the voltage drop profile in a real machine is more similar to the one shown in Fig. 1. That is, it has a rapid decrease right after the short-circuit is applied with a gradual return to V_{f0} . Furthermore, the error computed in this section considers a machine with the same parameters provided by the manufacturer, which is another approximation since the actual machine parameters may differ from these values.

Although the algorithm presented in this section used the manufacturer given values as the reference parameters, the actual machine parameters could be used when available.

The algorithm presented in this section can be used to indicate limits of field voltage variation so that the AC RMS component of the armature current can be used to recover the parameters from short-circuit tests of small size machines, being a partial solution for the problem mentioned in Section 3.2.

In addition, for large machines that do not face the problem mentioned in Section 3.2, the machine parameters can be obtained using either the VFVI or the CFVI model. The CFVI model may be chosen when the algorithm developed in this section indicates that the field voltage variations observed during the test do not influence significantly in the parameter identification.

5. Application

This section analyses the mathematical models developed in this paper. The VFVI model is tested in a 140 MVA synchronous machine that is subject to a short-circuit test with field voltage variation. This section also analyzes the performance of the CFVI model while determining the d-axis parameters in the same situation. Finally, the algorithm developed in Section 4 is used to determine the limits of field voltage variation for a maximum error of $\pm 15\%$ in the parameters computed by the CFVI model.

Section 5 uses data from a rated 13.8 kV, 50 Hz, 60-pole, 140 MVA synchronous machine described in Tables 1 and 2. The parameters described in Tables 1 and 2 are manufacturer's experimentally measured data, and thus are going to be considered as the actual machine parameters.

5.1. Recovering the machine parameters

In this section, the machine of Tables 1 and 2 is simulated during a short-circuit test while subject to an arbitrary field voltage variation. In this condition, the resultant armature current is used by the models CFVI and VFVI to recover the d-axis machine parameters. The results are summarized in Fig. 4 and Table 3.

In Fig. 4, the black dashed line represents the field voltage arbitrarily imposed during the sudden short-circuit test; V_{f0} was chosen so that, in the permanent state, the RMS value of the armature current was 0.58 p.u. In this figure, the dash-dot line (blue) represents the AC RMS

Table 1
Fundamental Parameters of The Machine (p.u.).

Parameter	Value (p.u.)	Parameter	Value (p.u.)
x_a	0.1431	x_Q	0.1054
x_{md}	0.9243	r_a	$2.688 \cdot 10^{-3}$
x_{kf}	-0.1195	r_D	$3.441 \cdot 10^{-2}$
x_D	0.7073	r_f	$4.305 \cdot 10^{-4}$
x_f	0.3230	r_Q	$1.504 \cdot 10^{-2}$
x_{mq}	0.5566		

Table 2
Derived Parameters of The Machine (p.u.).

Parameter	Value (p.u.)	Parameter	Value (s)
x_d	1.0670	τ_d'	2.421
\dot{x}_d	0.3099	τ_d''	$6.584 \cdot 10^{-2}$
x_d''	0.2352	τ_q''	$4.640 \cdot 10^{-2}$
x_q	0.6996		
x_q''	0.2317		

armature current for a short-circuit test with no field voltage variation. The continuous line (orange) represents the AC RMS armature current for the imposed field voltage variation; the data for this curve was obtained solving the differential Eqs. (a1) to (a13), which means that no approximation was made rather than the ones that naturally lead to these equations.

Finally, in Fig. 4, the dash-dot-dot line (red) is the nonlinear regression over the continuous line (orange) using the CFVI model, and the circles represent the nonlinear regression also made over the continuous line (orange) but using the VFVI model. In this last case, only a few samples of the regression were plotted in order to make the figure easier to understand.

From Fig. 4, it is possible to notice the significant influence that field voltage variations can have in the determination of d-axis parameters. Note that the mathematical model developed here matches the armature current determined by the solution of the differential Eqs. (a1) to (a13).

Table 3 presents the errors in the determination of the d-axis parameters by the CFVI and VFVI models when compared to the manufacturer's values presented in Table 2.

It can be seen that the armature current is better described by (6) than by (5) since the machine parameters can be better recovered using the VFVI model than by using the CFVI model.

5.2. Field voltage ride through

In this section, the model described in Section 4 is used to define limits of field voltage variation so that the CFVI model could provide results with absolute errors smaller than 15%, 10%, 5% and 1% for the machine described in Tables 1 and 2.

Fig. 5 shows four lines. The continuous line (black) limits the region where the field voltage can vary during the short-circuit test without imposing errors in the determination of the machine parameters higher than $\pm 15\%$ while using the CFVI model.

More specifically, this region goes from V_{f0} to the continuous black line, and it is represented by the hatched area. The first line above the continuous line limits the region of errors lower than $\pm 10\%$ (blue), the second line above the black continuous line limits the region of errors lower than $\pm 5\%$ (green), and the line closer to V_{f0} limits the region of errors lower than $\pm 1\%$ (red).

The initial field voltage adopted was chosen so that, in the permanent regime, the RMS value of the armature current was 0.58 p.u. It is interesting to note that the field voltage can be zero during 0.2 s and still the parameters obtained by the CFVI model would present errors smaller than $\pm 15\%$. The same goes for a voltage drop of 0.04 V_{f0} during 10 s.

In what concern the curves that limit errors lower than $\pm 10\%$, $\pm 5\%$, and $\pm 1\%$, it is possible to notice a significant decrease in the feasibility region of the field voltage from 0 to 10 s, while moving towards more restrictive limits of accuracy. It is also interesting to notice that the curve that limits the $\pm 1\%$ error region only allows field

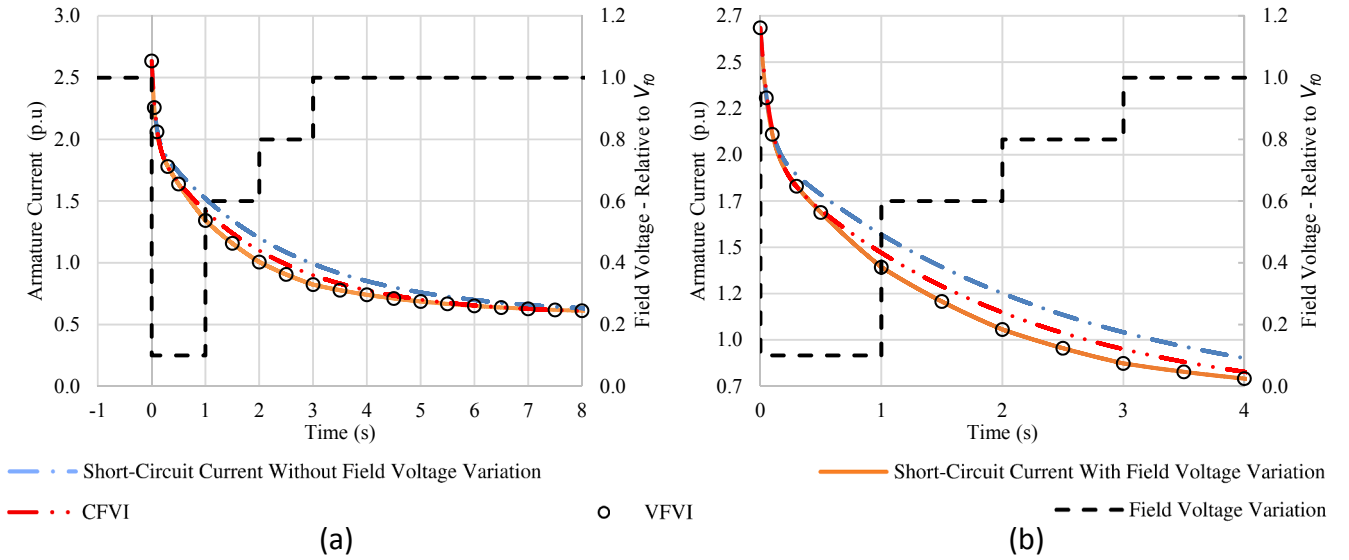


Fig. 4. The influence of field voltage variation on the performance of the CFVI and VFVI interpolation methods (a) and zoom from 0 to 4 s (b).

Table 3
Errors in the Parameter Computation.

Parameter	CFVI	VFVI
x_d	0.00%	0.00%
x_d'	2.98%	0.01%
x_d''	0.00%	0.00%
τ_d	-14.43%	0.01%
τ_d'	24.44%	0.08%

6. Conclusion

The short-circuit test is a procedure widely used in the determination of d-axis parameters of synchronous machines. In IEEE Std. 115, a special emphasis is put on the precautions to be taken with field voltage variations during this test. Also, remarks on the importance of low-impedance excitation systems and low field voltage variations are common in the main standards. However, no variation limits are specified. Moreover, there is not much research about the impacts of these variations in the parameter accuracy.

This paper makes a deep analysis of the field voltage variation impact in the determination of d-axis parameters of synchronous machines using the short-circuit test. A mathematical model is developed that can recover the machine parameters very efficiently and with high accuracy even when field voltage variations are presented during the short-circuit test.

In addition, this paper proposed an algorithm that defines limits of field voltage variations in order to respect a certain parameter estimation uncertainty while using the traditional interpolation methods that do not consider field voltage variation.

Future work should investigate the performance of the VFVI method in machines of different sizes, identifying the limits where the AC RMS component cannot be used to recover the machine parameters from short-circuit tests with field voltage variations.

Also, future work should incorporate a certain margin of variability in the parameters provided by the manufacturer, while determining the limits of field voltage variation as described in Section 4. This would provide more conservative limits that could be used in practice or incorporated in the standards.

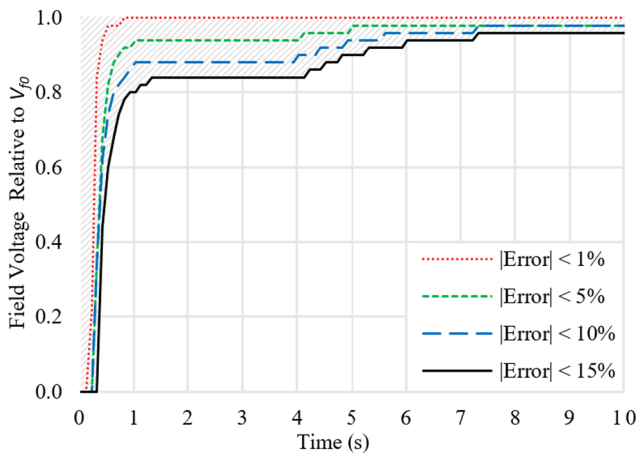


Fig. 5. Limits of field voltage variation for a maximum error of 15%, 10%, 5% and 1% in the estimated parameters.

voltage variations that last for less than 1 s. Also, for the limit of $\pm 1\%$ error, the field voltage can go to zero during about 50 ms so that the estimation of the machine parameters are not affected in more than 1% while using the CFVI model.

Appendix

In this section, a brief proof of expression (2) is given. Even though the proof made here considers only one damper winding, it is possible to arrive at a similar expression if unlimited dampers are considered. In this last case, one must incorporate these windings in the operational impedances of the machine and proceed to a similar deduction as done here.

In the deductions made here, i indicates current in the time domain, and I indicates current in the frequency domain. The reference frame used in this work is described below together with the correspondent synchronous machine equations [20].

For the reference frame described in (a1) to (a3) $\mathcal{P}^{-1} = \mathcal{P}'$, the inverse of \mathcal{P} is equal to its transpose; $\gamma_{0,d,q}$ represents any quantities in the $0dq$ reference; and $\gamma_{a,b,c}$ represents any quantities in the abc stator reference frame. For more information refer to [20].

$$\begin{bmatrix} \gamma_0 \\ \gamma_d \\ \gamma_q \end{bmatrix} = \sqrt{\frac{2}{3}} \mathcal{P} \begin{bmatrix} \gamma_a \\ \gamma_b \\ \gamma_c \end{bmatrix} \quad (\text{a1})$$

$$\mathcal{P} = \begin{bmatrix} 1/\sqrt{2} & 1/\sqrt{2} & 1/\sqrt{2} \\ \cos(\theta) & \cos(\theta - 2\pi/3) & \cos(\theta + 2\pi/3) \\ \sin(\theta) & \sin(\theta - 2\pi/3) & \sin(\theta + 2\pi/3) \end{bmatrix} \quad (\text{a2})$$

$$\theta(t) = \omega t + \frac{\pi}{2} + \delta \quad (\text{a3})$$

Finally, the machine equations are described in (a4) to (a13).

$$\psi_d(t) = (x_{md} + x_a)i_d(t) + x_{md}i_f(t) + x_{md}i_D(t) \quad (\text{a4})$$

$$\psi_q(t) = (x_{mq} + x_a)i_q(t) + x_{mq}i_Q(t) \quad (\text{a5})$$

$$\psi_f(t) = x_{md}i_d(t) + (x_{md} + x_{kf} + x_f)i_f(t) + (x_{md} + x_{kf})i_D(t) \quad (\text{a6})$$

$$\psi_D(t) = x_{md}i_d(t) + (x_{md} + x_{kf})i_f(t) + (x_{md} + x_{kf} + x_D)i_D(t) \quad (\text{a7})$$

$$\psi_Q(t) = x_{mq}i_q(t) + (x_{mq} + x_Q)i_Q(t) \quad (\text{a8})$$

$$v_d(t) = -r_a i_d(t) - \frac{\dot{\psi}_d(t)}{\omega} - \psi_q(t) \quad (\text{a9})$$

$$-v_f(t) = -r_f i_f(t) - \frac{\dot{\psi}_f(t)}{\omega} \quad (\text{a10})$$

$$0 = -r_D i_D(t) - \frac{\dot{\psi}_D(t)}{\omega} \quad (\text{a11})$$

$$v_q(t) = -r_a i_q(t) - \frac{\dot{\psi}_q(t)}{\omega} + \psi_d(t) \quad (\text{a12})$$

$$0 = -r_Q i_Q(t) - \frac{\dot{\psi}_Q(t)}{\omega} \quad (\text{a13})$$

Substituting $v(t)$ and $i(t)$ by (a14) to (a15) in the equations (a4) to (a13), where $v(\infty)$ and $i(\infty)$ represents the voltage and current steady state values. Also, simplifying the results and writing them in the frequency domain yields (a16) to (a19). Here it is going to be assumed that the step ΔV_f in the field voltage happens in $t = 0$ but nothing restricts us of generalizing the results for steps in $t \neq 0$.

$$\Delta v(t) = v(t) - v(\infty) \quad (\text{a14})$$

$$\Delta i(t) = i(t) - i(\infty) \quad (\text{a15})$$

$$\mathcal{L}\{\Delta v(t)\} = s\Delta V \quad (\text{a16})$$

$$\mathcal{L}\{\Delta i(t)\} = s\Delta I \quad (\text{a17})$$

$$\Delta V_d = -r_a \Delta I_d - s \frac{X_d(s) \Delta I_d + G(s) \Delta V_f}{\omega} - X_q(s) \Delta I_q \quad (\text{a18})$$

$$\Delta V_q = -r_a \Delta I_q - s \frac{X_q(s) \Delta I_q}{\omega} + X_d(s) \Delta I_d + G(s) \Delta V_f \quad (\text{a19})$$

For an unexcited synchronous machine ($V_{f0} = 0$) rotating at synchronous speed that in $t = 0$ is short-circuited $\Delta V_d = \Delta V_q = 0$. Given that also in $t = 0$ a step of magnitude $V_{\Delta f}$ is applied in the field voltage $\Delta V_f = V_{\Delta f}/s$.

Neglecting the terms with r_a except for α , and solving (a18) to (a19), yields (a20) to (a21).

$$I_d = \frac{-V_{\Delta f} \frac{(s^2 + \omega^2)G(s)}{X_d(s)}}{s(s^2 + 2s\alpha + \omega^2)} = \frac{-V_{\Delta f} H(s)}{(s^2 + 2s\alpha + \omega^2)} \quad (\text{a20})$$

$$I_q = 0 \quad (\text{a21})$$

$$H(s) = \frac{A}{(s\tau_d + 1)} + \frac{B}{(s\tau_d + 1)} + \frac{C}{s} + D \quad (\text{a22})$$

$$A = \frac{-\omega^2 \tau_{db} \tau_d'^2 + \omega^2 \tau_d'^3 - \tau_{db} + \tau_d'}{\tau_d' (\tau_d' - \tau_d')} \quad (\text{a23})$$

$$B = \frac{\omega^2 \tau_{db} \tau_d''^2 - \omega^2 \tau_d''^3 + \tau_{db} - \tau_d''}{\tau_d'' (\tau_d'' - \tau_d'')} \quad (\text{a24})$$

$$C = \omega^2 \quad (\text{a25})$$

$$D = \frac{\tau_{db}}{\tau_d'' \tau_d''} \quad (\text{a26})$$

$$\tau_{db} = \frac{x_D}{\omega r_d} \quad (\text{a27})$$

$$\alpha = \frac{\omega r_a}{2} \left[\frac{1}{X_d(s)} + \frac{1}{X_q(s)} \right] \approx \frac{\omega r_a}{2} \left(\frac{1}{x_d} + \frac{1}{x_q} \right) \quad (\text{a28})$$

A translation from the frequency domain to the time domain is now performed. The expressions (a29) and (a30) are used as they represent a good approximation for the problem handled here since a and α are much less than ω [12]. From the expression (a20) to the expression (a31) using (a29) and (a30), it is important to notice that the values of a depend only on the denominators of the sums in (a22). For the first sum in (a22) $a = 1/\tau_d''$, for the second sum $a = 1/\tau_d''$, for the third sum $a = 0$. The fourth sum uses the expression (a30).

$$\mathcal{L}^{-1} \left\{ \frac{\omega^2}{(s+a)(s^2+2s\alpha+\omega^2)} \right\} \approx e^{-at} - e^{-\alpha t} \cos(\omega t) \quad (\text{a29})$$

$$\mathcal{L}^{-1} \left\{ \frac{\omega}{(s^2+2s\alpha+\omega^2)} \right\} \approx e^{-\alpha t} \sin(\omega t) \quad (\text{a30})$$

$$i_d = \frac{-V_{\Delta f} x_{md}}{r_f x_d \omega^2} \left(\frac{A}{\tau_d''} e^{-\frac{t}{\tau_d''}} + \frac{B}{\tau_d''} e^{-\frac{t}{\tau_d''}} + C \right) + \frac{V_{\Delta f} x_{md}}{r_f x_d \omega^2} e^{-\alpha t} \left[\left(\frac{A}{\tau_d''} + \frac{B}{\tau_d''} + C \right) \cos(\omega t) - D \sin(\omega t) \right] \quad (\text{a31})$$

Assuming that τ_d'' is significantly larger than τ_d'' and τ_{db} , it is possible to make the following approximations (a32) to (a35).

$$\frac{A}{x_d \tau_d'' \omega^2} \approx \frac{\tau_d'' + \frac{1}{\tau_d'' \omega^2}}{-\tau_d'' x_d} \approx -\frac{1}{x_d} \quad (\text{a32})$$

$$\frac{B}{x_d \tau_d'' \omega^2} \approx \frac{\frac{\tau_d'' - \tau_{db}}{\tau_d''} - \frac{1}{(\tau_d'' \omega^2)} \frac{\tau_{db} \tau_d''}{\tau_d''}}{x_d} \approx 0 \quad (\text{a33})$$

$$\frac{D}{x_d \omega} = \frac{1}{x_d} \frac{\tau_{db}}{\tau_d''} \frac{1}{\tau_d'' \omega} \approx 0 \quad (\text{a34})$$

$$i_d = -\frac{V_{\Delta f} x_{md}}{r_f x_d} \left(1 - e^{-\frac{t}{\tau_d''}} \right) \quad (\text{a35})$$

Using the expression (a36), it is possible to move from a rotor reference frame to a stator reference frame.

$$i = \sqrt{2/3} [-i_d \sin(\omega t + \theta_0) + i_q \cos(\omega t + \theta_0)] \quad (\text{a36})$$

$$i = \sqrt{\frac{2}{3}} \frac{V_{\Delta f} x_{md}}{r_f x_d} \left(1 - e^{-\frac{t}{\tau_d''}} \right) \sin(\omega t + \theta_0) \quad (\text{a37})$$

Finally, the expression (a37) can be extended to a step applied in an instant T_i (a38).

$$i_{\Delta f}^i = \sqrt{\frac{2}{3}} \frac{x_{md} V_{\Delta f}}{x_d r_f} \left(1 - e^{-\frac{t-T_i}{\tau_d''}} \right) \sin(\omega t + \theta_0) U(T_i) \quad (\text{a38})$$

References

- [1] Krause P, Wasynchuk O, Pekarek S. *Electromechanical Motion Devices*, 2nd ed. IEEE Press series on Power Engineering, John Wiley & Sons, Inc., New Jersey. 2012.
- [2] Kundur P, Paserba J, Ajarapu V, Andersson G, Bose A, Canizares C, et al. Definition and classification of power system stability IEEE/CIGRE joint task force on stability terms and definitions. *IEEE Trans Power Syst* 2004;19(3):1387–401.
- [3] W. A. Elmore, *Protective Relaying Theory and Applications*, 2nd ed. New York: Marcel Dekker, 2004.
- [4] Adrees A, Milanović V. Optimal compensation of transmission lines based on minimization of the risk of subsynchronous resonance. *IEEE Trans Power Syst* 2016;31(2):1038–47.
- [5] IEEE Guide for Test Procedures for Synchronous Machines Part II—Test Procedures and Parameter Determination for Dynamic Analysis, IEEE Std. 115, 2009.
- [6] Escarela-Prez R, Niewierowicz T, Campero-Littlewood E. Synchronous machine parameters from frequency response finite-element simulations and genetic algorithms. *IEEE Trans Energy Convers* 2001;16(2):198–203.
- [7] Bortoni EC, Jardini JA. Identification of synchronous machine parameters using load rejection test data. *IEEE Trans Energy Convers* 2002;17(2):242–7.
- [8] Bortoni EC, Bernarders Jr JV, Araujo BT, Silva PVV. Revisiting three-phase sudden short-circuit and voltage recovery tests. *Electric Machines and Drives Conference (IEMDC)*. 2017.
- [9] Martin JP, Tindall CE, Morrow DJ. Synchronous machine parameters determination using the sudden short-circuit axis currents. *IEEE Trans Energy Convers* 1999;14(3):454–9.
- [10] Oliveira SEM, Souza JA. Effect of field-voltage source impedance on load-rejection test results of large-rating synchronous generators. *IEEE Trans Energy Convers* 2011;26(1):30–5.
- [11] Rodríguez GG, Silva AS, Zeni N. Identification of synchronous machine parameters from field flashing and load rejection tests with field voltage variation. *Electr Power Syst Res* 2017;143:813–24.

- [12] P.C. Krause, O. Wasynczuk, and S.D. Sudhoff, *Analysis of Electric Machinery and Drive Systems*, 3rd ed, Wiley-IEEE Press, 2002.
- [13] Fonseca JS, Coelho CU, Bortoni EC. *Wireless sensor for field quantities measurement in brushless synchronous machines*. Proceedings of the PESGM. 2017.
- [14] Kamwa I, Carle H, Viarouge P, Mpanda-Mabwe B, Crappe M. *Computer software to automate the graphical analysis of sudden-short-circuit oscillograms of large synchronous machines*. IEEE Trans Energy Convers 1995;10(3):399–406.
- [15] Araujo BT, Bernardes Jr JV, Bortoni EC, Lambert-Torres G. *Synchronous machine parameters evaluation with a hybrid particle swarm optimization algorithm*. Electr Power Compon Syst 2017;45(17):1962–71.
- [16] Hutchison G, Zahawi B, Giaouris D, Harmer K, Stedall B. *Parameter estimation of synchronous machines using particle swarm optimization*. Proceedings of the PMAPS. 2010.
- [17] Silva PVV, Bortoni EC, Rocha JJ. *Identification of Synchronous Machines Parameters using Genetic Algorithm and Load Rejection Test*. Proceedings of the PESGM. 2017.
- [18] AMPL. *A Modeling Language for Mathematical Programming*. [Online] Available: <http://www.ampl.com>.
- [19] Artelys Knitro. *Artelys Knitro–Nonlinear optimization solver*. [Online]. Available: <https://www.artelys.com>.
- [20] Anderson PM, Fouad AA. *Power System Control and Stability*. 3rd ed, IEEE Press series on Power Engineering, John Wiley & Sons, Inc., New Jersey. 2003.